An earlier version appeared in: *11th International Symposium on Fireworks* (2009).

A New Aerial Shell Ballistic Model Experimentally Verified

L. Weinman Schneier/Weinman Consultants
Austin, TX, USA Lawrence@Weinman.Net
K. L. & B.J. Kosanke Pyrolabs, Inc.
Pyrolabs, Inc., Whitewater, CO, USA
and
J. Widmann Connecticut Pyrotechnic Manufacturing Inc.
Connecticut Pyrotechnic Manufacturing Inc., Sandy Hook, CT, USA

ABSTRACT

The authors present models that predict fireworks shell trajectories and validate them with experimental data.

Introduction

Early in 2008, the authors began a series of ballistics field trials to validate two computer models and, if the models proved to be valid, to use them to provide guidance to both firework display operators and AHJs when attempting to determine appropriate spectator separation distances for firework displays using off-vertical angled mortars and/or when launching displays from elevated sites. For these field trials, spherical shells were selected for three reasons; a) at present they are the most common type used in firework displays, b) the treatment of their aerodynamic properties is much simpler than for cylindrical shells, and c) their drag is typically lower than that for cylindrical shells and, as a result, their range is typically greater than that of cylindrical shells and therefore the results will be conservative.

Methods

The methods used in this study involved:

a) The use of specially prepared dummy aerial shells, in two different diameters, each complete with a 'dummy' fuse to better simulate actual spherical firework shells.

b) A statistical treatment of the mean flight times and impact locations of the shells.

c) The calibration of the model using the muzzle velocities of the launched shells, their flight times and the ground impact locations, and the properties of the local atmosphere at the time of launch.

The Shells and Data Collection

The shell diameters chosen were those for typical/nominal 3-inch (76 mm) and 6-inch (155 mm) shells. Each of the dummy shells contained a small neodymium-based permanent magnet and each group of shells was constructed to be carefully matched for size and mass. The masses for each size were chosen to be at or slightly below the minimum typical mass for such diameter, and similarly, at or slightly above the typical maximum mass for such a diameter. Thus, there were 4 different types of dummy shells used. Furthermore, the lift (i.e., propelling) charges were also varied over a range expected to produce velocities somewhat exceeding the expected velocity range for actual shells used in firework displays.

The actual diameters of the 3-inch and 6-inch shells were 2.80 inches (71 mm) and 5.35 inches (136 mm), respectively. The masses of the 3-inch test shells ranged from 91 g to 93 g and from 169 g to 174 g for the light and heavy shells, respectively, whereas the masses of the 6-inch shells ranged from 803 g to 851 g and 1227 g to 1237 g for the light and heavy shells, respectively. This range of values is believed to adequately cover the expected density range for typical aerial shells.

The lift charges were varied so as to produce launch velocities for the dummy shells ranging from slightly less than 60 m/s (200 fps) to nearly 120 m/s (400 fps). The off-vertical launch angles

used ranged from approximately 5° to 30°. In all, 85 shells of various masses, velocities, diameters and off-vertical angles were test fired.

The shells were fired from a mortar held in a well-constructed frame that could be adjusted for off-vertical angle, shown in Figure 1. The frame also held the two coils that were used to determine the velocity at which the shells were launched. The coils generate a voltage when the magnetic fields of the shell's internal magnets pass through them. The voltage profiles from such an interaction are shown in Figure 2. These wave forms are easily converted to a highly accurate velocity value with little uncertainty, as the time determinations are made at the easily measurable zero crossing points. The expected accuracy of this method for the highest velocities was within +/– 0.4%, with the lower velocities being more accurately determined.

Figure 1. Mortar mounted on frame.

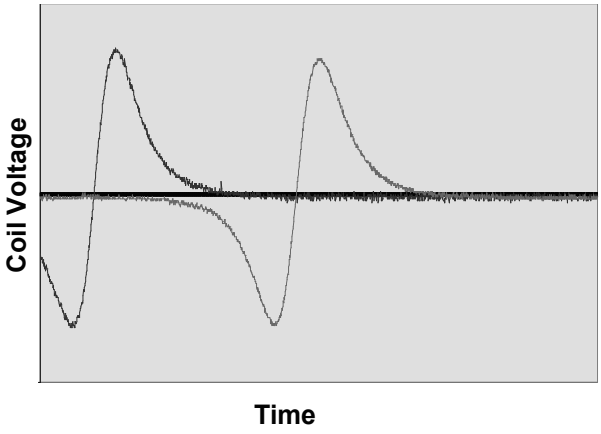

Figure 2. Voltage profiles.

The location of the launch point and the points of impact were determined using a Global Positioning System (GPS) device that could locate these points within approximately +/– 7 ft (~ 2 m). The total flight times were determined by two observers using stop watches, observing the time of launch and listening for the sound of impact. In each case, a correction was made for the speed of sound from the point of impact to the location of the observers. These times are estimated to be within +/– 0.25 s.

The Statistics from Data Reduction

The data collected were then analyzed to yield the times of flight and the distance from the launch point to the impact points. An example of two sets of the data is shown in Figure 3. The pairs of circles indicate, for each shell mass group, the mean distance and the mean plus 2.03 standard deviations. The choice of 2.03 standard devia-

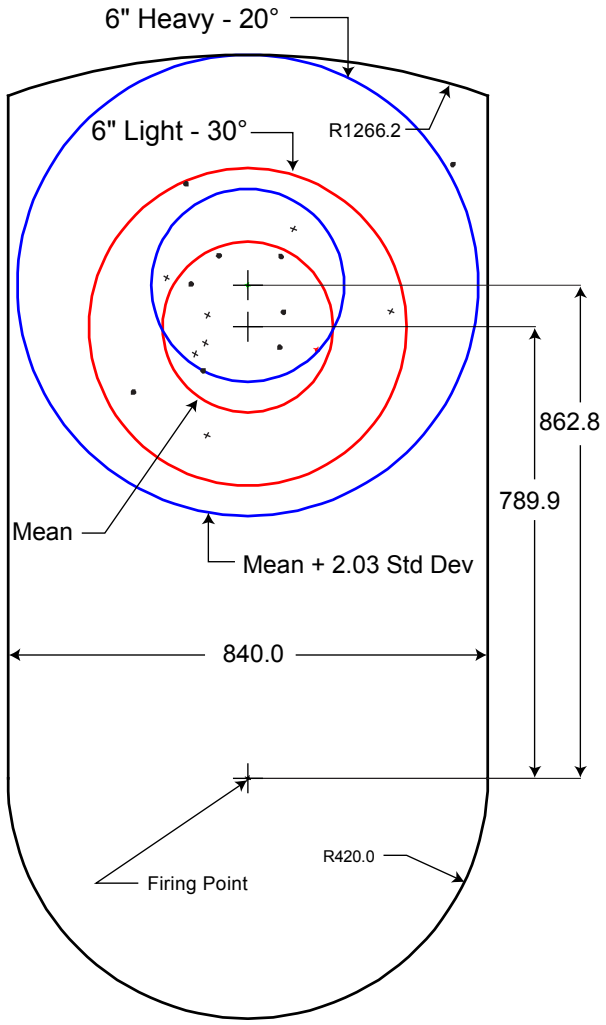

Figure 3. A plot showing the impact points for both low and high mass 155 mm (6") shells fired at off-vertical angles of 20 and 30°.

tions will, for normally distributed data, give a probability of impact within that circle of 95%, which was seen to be the case for all tests. All of the shell plots are generally similar in that the deviations across the line of fire are less than along the line of launch, and generally the deviations across, although similar, are also less than the present standard NFPA 1123 standard of 70 feet per inch (0.84 m/mm or 8.4 m/cm) of nominal shell diameter. This data, along with the times of flight and launch angles were then used to evaluate the 2 models that the authors have written. The models are actually quite similar, with the older one using an average drag coefficient and a simplified estimate of the properties of the atmosphere, and the newer model using a velocity dependent drag coefficient and more detailed properties of the atmosphere. The results are as expected with the newer model yielding somewhat more accurate estimates of the experimentally determined times of flight and impact distances.

The New Ballistic Model

There are two types of trajectories that could be considered. The first is generally referred to as the 'vacuum' trajectory. In this case, it is assumed that the only force acting on the shell during its flight is that of gravity. However, this is very unrealistic and would only be suitable for a classroom introduction. The second can be called the 'real world' trajectory. In this case, the forces that act on the shell are gravity and the aerodynamic forces produced by its motion through the surrounding fluid, which is air. It is the consideration of the aerodynamic forces that complicates the computation of a real world trajectory.

For modeling purposes, the aerial shell travelling through the air is a more or less rough and imperfect sphere. The derivation of a mathematical model has, in the past, been the subject of great mystery and supposed complication. However, in practice, it need rely on nothing other than simple algebra, utilizing only the following equations:

1) Acceleration = Force / Mass

2) Velocity = Acceleration × Time

3) Distance = Velocity × Time

4) Drag force = Cd × 0.5 × ρ × V^2 × Area

Furthermore, one might consider the first three equations as trivial Newtonian mechanics. It is only the fourth equation that may be unfamiliar, and that has more to it than first meets the eye.

In Equation 4, the area is a constant since, at least for a dud shell, it does not change during the flight. The velocity (V) is a computed value based on the initial velocity at the time of launch, and the combined gravitational and aerodynamic forces that affect the subsequent velocity. The complication must then arise from the other two parameters, the density of the air along the trajectory (ρ), and the drag coefficient (Cd).

Collectively then, the force exerted on the sphere travelling through air, as given in Equation 4, is a function of the geometry of the object, the properties of the air, and the relative velocity of the sphere to that of the air. This force along with that of gravity act to change the velocity, and direction, of the sphere with time. Very simply put, the effective force on the sphere is the product of gravity, the size and geometry of the sphere, the mass and velocity of the sphere, the properties of the air, and a number called the drag coefficient (Cd).

In order to develop an understanding of why large and small objects, which are otherwise similar, seem to have different characteristics while moving through a fluid, such as air, some way is needed to characterize the 'similarity' of such objects and fluids. In the late 1800s, Osborne Reynolds noticed that a ratio of the inertial forces to the viscous forces (now called the Reynolds number) would allow that. Simply put, some object moving through a fluid with the same calculated Reynolds number, will behave similarly to that of some otherwise similar, but larger or smaller object, moving through another fluid and having the same calculated Reynolds number.

The drag coefficient is empirically derived from test data, and that for (nearly perfect) spheres takes the values indicated in Figure 4. Notice that the plot uses the Reynolds number as one axis where the Reynolds number (Re) is given by

$$\mathrm{Re} = \frac{V \times L}{\mu/\rho} \quad \left[\mu/\rho \text{ is the kinematic viscosity "}v\text{"}\right]$$

where, V is the object's velocity, L is a parameter called 'characteristic length' (which in the case of a sphere is its diameter), μ is the absolute viscosity of the fluid (in this case the local air), and ρ is the density of the fluid, again the air. The Reynolds number, therefore, varies with the size of the moving object, the velocity of the object, and the local

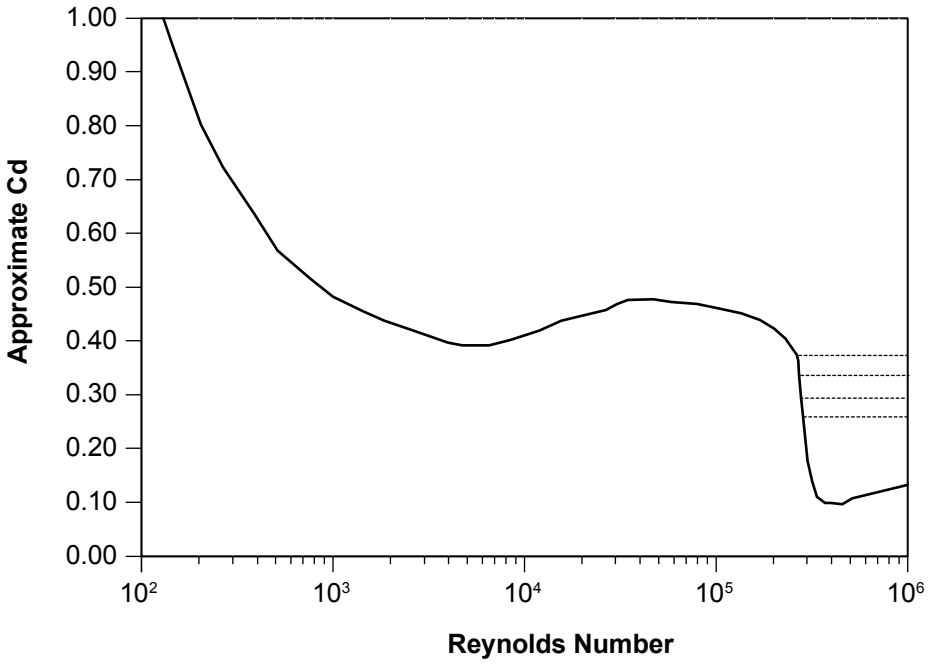

Figure 4. Approximate coefficient of Drag as a function of Reynolds Number.

and immediate properties of the fluid (air). It has the useful feature of allowing different sized items, but of similar geometry, to be directly compared.

Past models have generally, but not always, included a means to determine the air density based on some standard value at the launch altitude. However, the density of the air (even in a gross sense, and aside from its standard molecular composition) is also dependent on the local pressure, the local temperature and the humidity. Because the drag coefficient varies significantly with the Reynolds number, lookup tables were incorporated in the present model, both for the values of μ as a function of temperature and for *Cd* as a function of the Reynolds number.

If the sphere were 'ideal', meaning that it was perfectly spherical and very smooth (i.e., highly polished), it would have a relationship of *Cd* vs. Reynolds number as shown in Figure 4. However, spherical firework shells are neither sufficiently round nor sufficiently smooth to exactly match the empirical data from carefully controlled wind tunnel experiments. What this lack of sphericity and smoothness does is effectively to move the abrupt 'break' which occurs at about a Reynolds number of 300,000 to some lower number, and where the decrease in *Cd* approximately levels off to a value typically between 0.2 and 0.4. This is indicated in the above graph by the dashed lines, although in practice the transition is smoother. As far as the authors are aware, all previous aerial shell ballistic models utilized a fixed *Cd*.

Figure 5 shows sets of calculated Reynolds numbers for two different diameter, perfect spheres as a function of time in seconds for hypothetical aerial shell launches. As can be readily seen, using some fixed *Cd* for shells would not be a correct thing to do, as the *Cd* varies over a wide range during the flight, especially for aerial shells launched under a wide variety of conditions.

The present model does a simple iteration over time for the velocity and 2-dimensional positioning of an aerial shell, but also frequently updates all the atmosphere properties information based on a set of initial conditions and accepted values for the standard atmosphere.

Model Calibration

The mean flight time and impact location point data from the firing test sets was used as input to the model, along with all the relevant atmospheric information. The internal calculated values were then optimized for each data set. These mean calculated values for *Cd* versus Reynolds number were then utilized over all the input test sets.

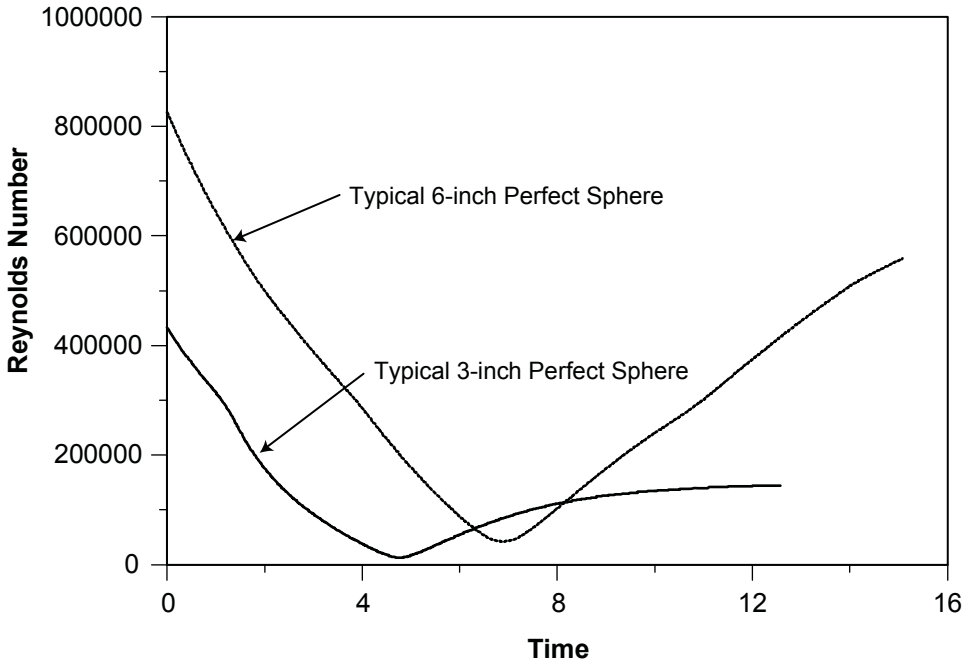

Figure 5. Perfect 76 mm (3") and 155 mm (6") spheres launched near vertical and with masses and velocities typical of aerial shells

Model Results

One test set that did not seem to match the others as closely as was expected. If that test set is included in the calibration calculations, the prediction of the mean impact points and flight times is within 3.04% for distance and 1.02% for time. However, if that test set is excluded from the calibration calculations, the prediction from the model is within 0.83% for distance and 0.68% in time for all other test sets.

The calibrated models can be used to predict the flight of shells within certain limitations. The shells used in this study were selected to correspond to most of the shells used in typical firework displays. However, the models are thought to be sufficiently accurate to successfully predict the trajectories for shells up to 205 mm (8") and to off-vertical angles of up to something over 30°, as these are not too far from the actual tested parameters. Nonetheless, the authors warn that using any model to extrapolate at extremes from the actual experimental data is never warranted without caution. Figures 6 to 14 are for 76 mm (3") and 155 mm (8") hypothetical aerial shells having actual diameters of 69 mm (2.7") and 193 mm (7.6"), respectively. If not otherwise specified, the velocity of launch was assumed to be 91 m/s (300 ft/s) and the masses are given in Table 1.

Table 1. Shell masses.

Shell Type	Shell Mass (g)	
	76 mm	205 mm
Light	103.2	2298.4
Average	129.0	2873.0
Heavy	154.8	3447.6

It should be noted that the 'mean' values of elevation and temperature are the mean values for the average altitude of the United States' lower 48 states and the recent average annual temperature (2500 ft above sea level and 59° F at sea level). The 'Altitude from Mortar' axis extends to –1000 feet (below the launch site) so that the information may be used for launches from elevated sites. Additional information is given for more extreme conditions, and, as can be seen, may result in significant changes in the expected impact distances. Furthermore, the modeled distances are just that and may not match the values for any specific aerial shell.

Wind effects

While the model presently incorporates a method for dealing with the effects of wind on

aerial shells, it is not presented here since the authors had no reasonable way to properly calibrate the model for those effects. This is exacerbated by the variable, and mostly unknown, magnitudes and directions of any wind more than slightly above ground level. While information on 'average' winds aloft may sometimes be available, the short duration of an aerial shell flight requires more contemporaneous, and exact, information than is usually available.

There also seems to be some contention between this and other model results and users anecdotal evidence for the actual effects of wind. Absent any accurate real world testability, we believe that it would be improper to present any such wind effects results.

References

1) *Boundry Layer Theory*, Hermann Schlichting, 7th ed., McGraw Hill, 1979.

2) *Airplane Aerodynamics*, Dommasch, Sherby, Connolly, 4th ed., Pitman Publishing, 1967.

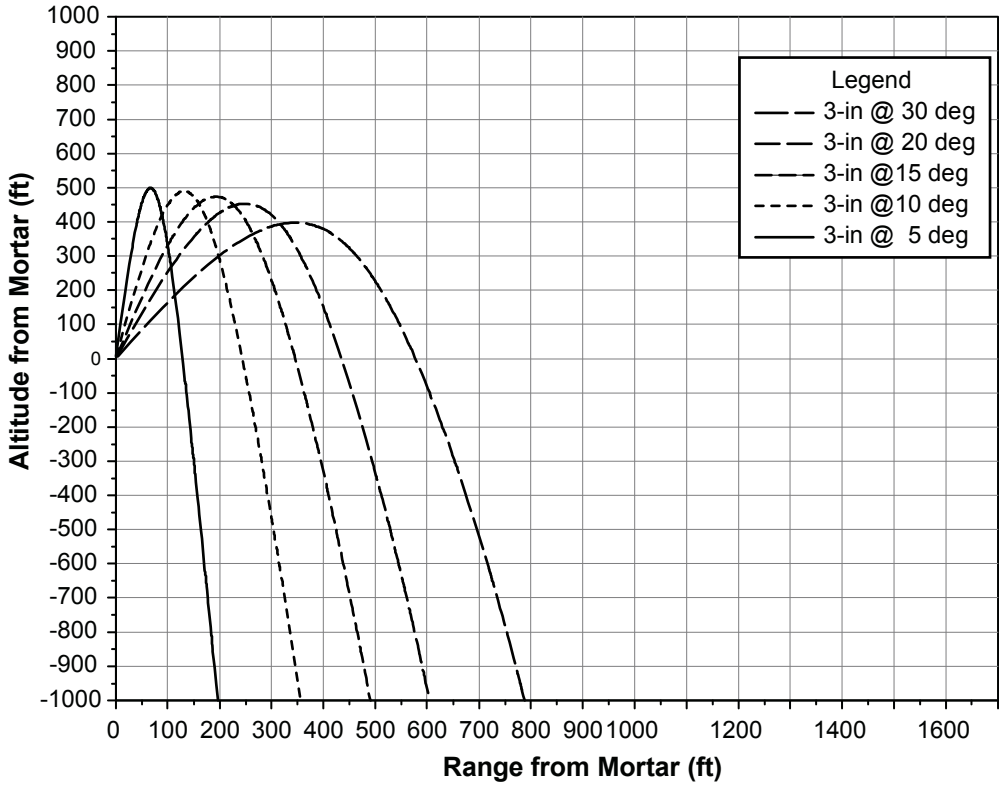

Figure 6. Trajectories for 76 mm (3") shell (2500 ft above sea level, 50° C, 50% RH).

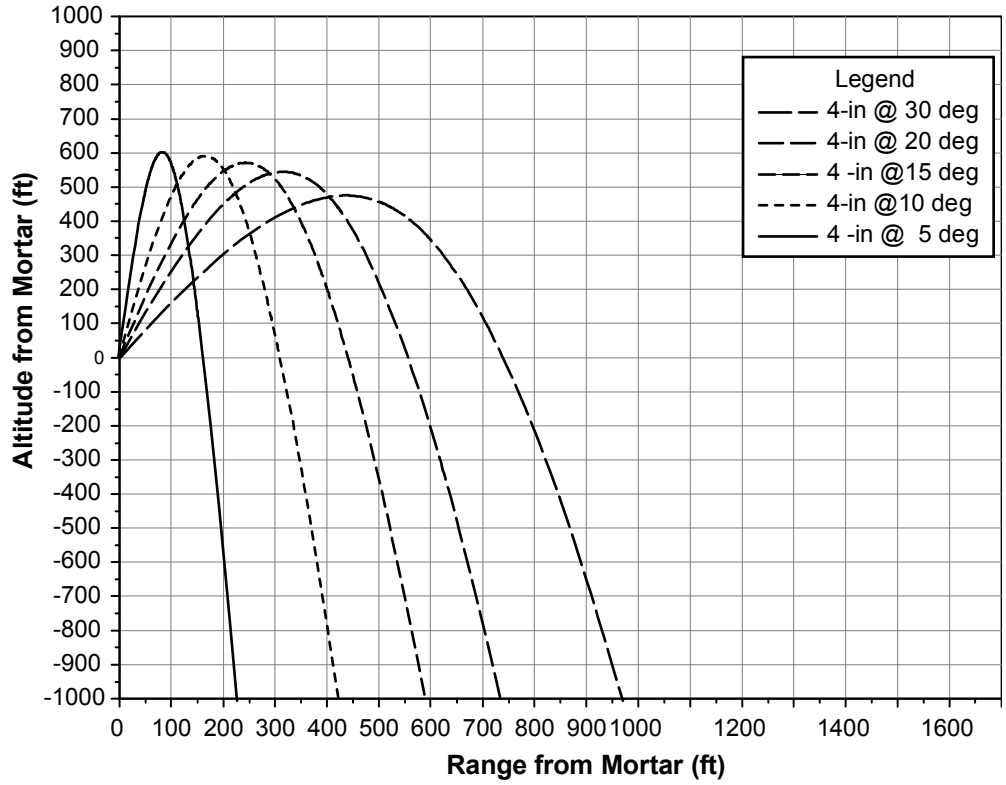

Figure 7. Trajectories for 101 mm (4") shell (2500 ft above sea level, 50° C, 50% RH).

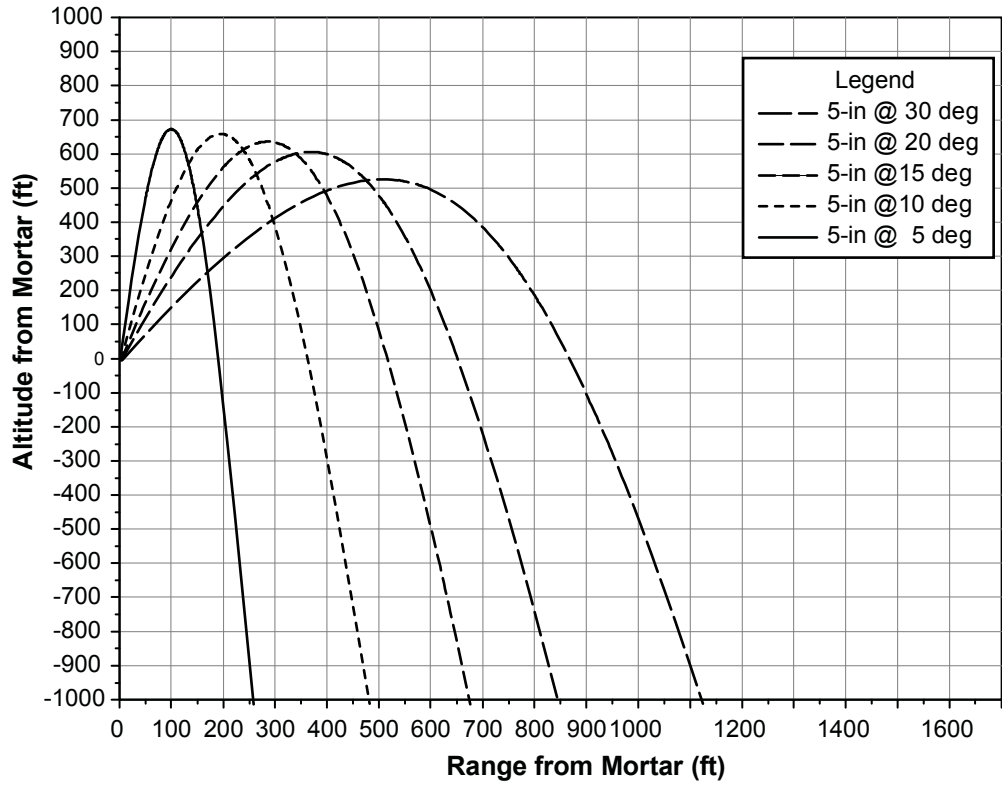

Figure 8. Trajectories for 127 mm (5") shell (2500 ft above sea level, 50° C, 50% RH).

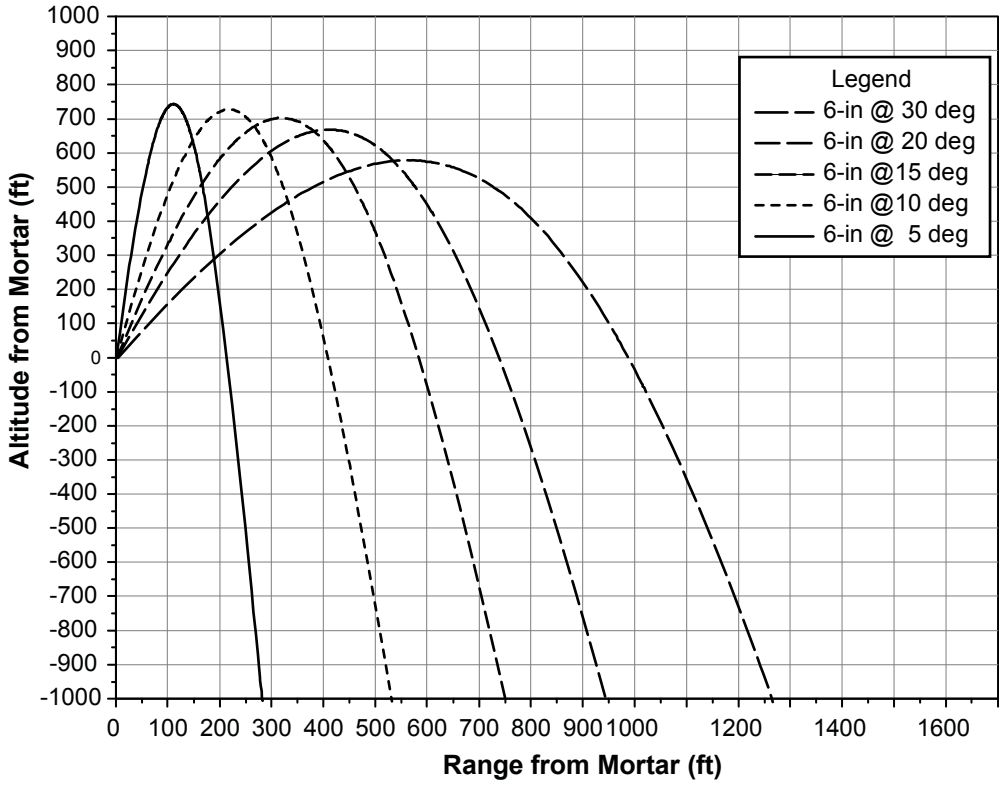

Figure 9. Trajectories for 155 mm (6") shell (2500 ft above sea level, 50° C, 50% RH).

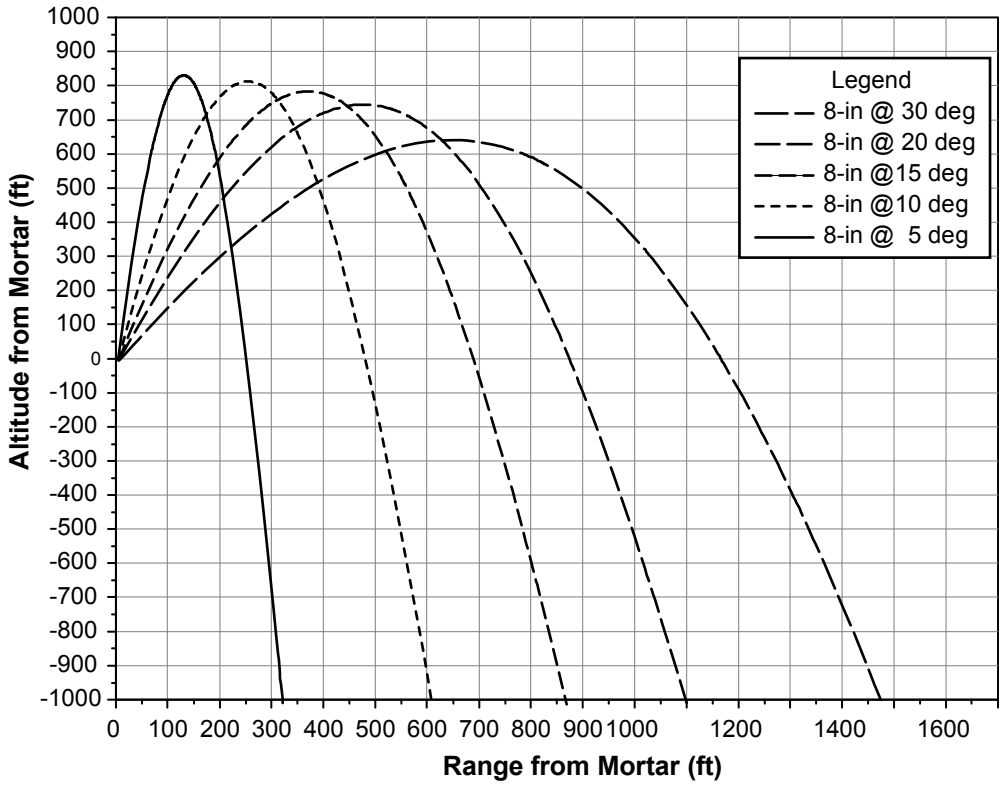

Figure 10. Trajectories for 205 mm (8") shell (2500 ft above sea level, 50° C, 50% RH).

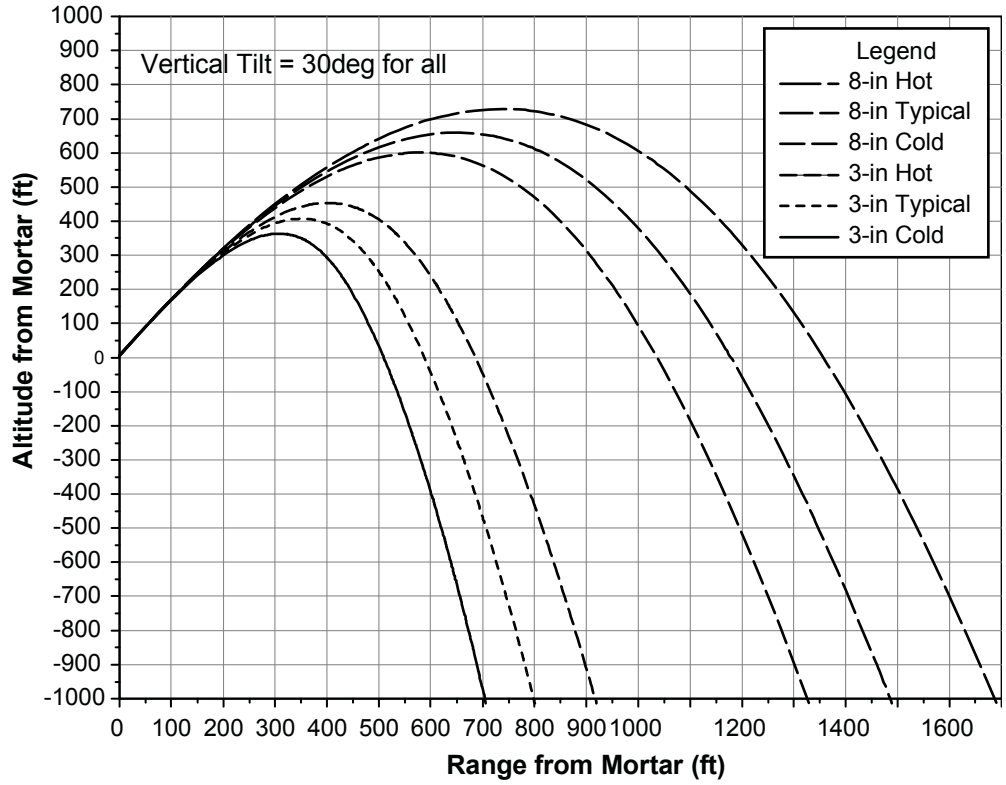

Figure 11. Comparison of trajectories for 76 and 205 mm (3 and 8") shells at extreme temperature and altitude.

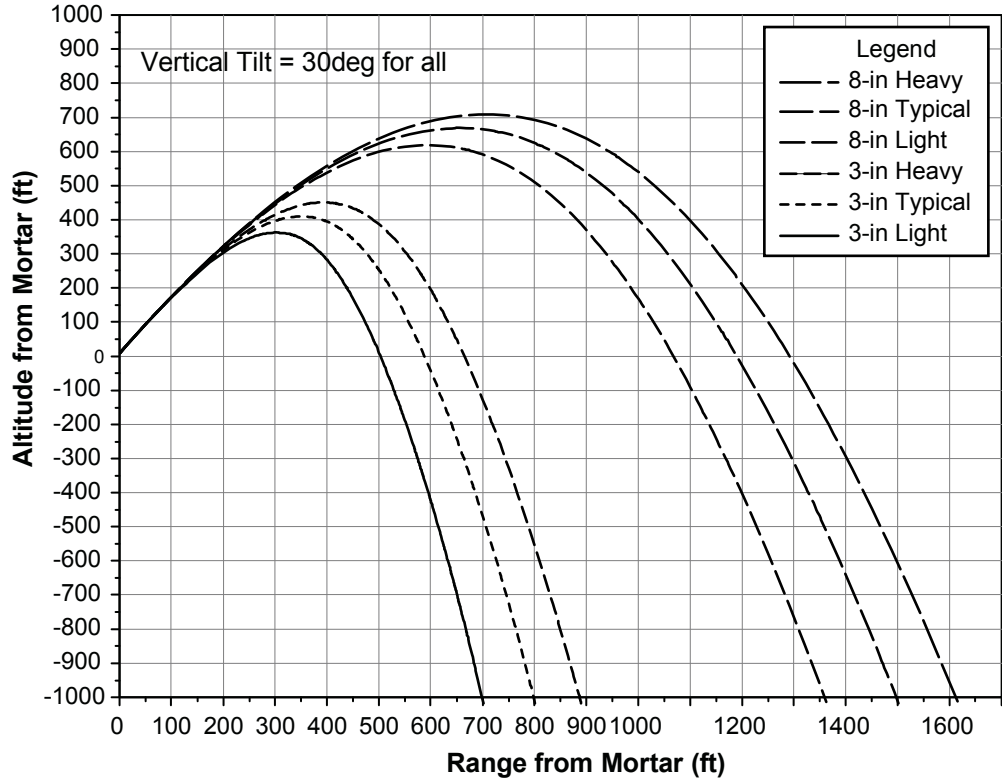

Figure 12. Comparison of trajectories for 76 and 205 mm (3 and 8") of three different masses (–20%, typical and +20%) (2500 ft above sea level, 50° C, 50% RH).

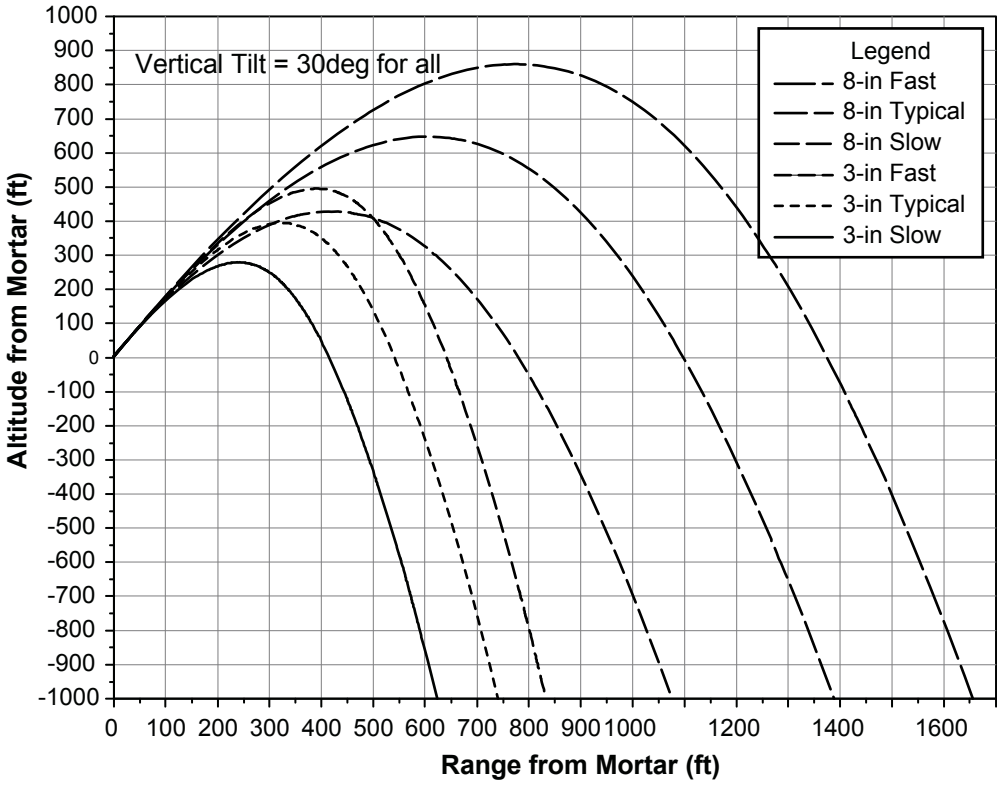

Figure 13. Comparison of trajectories for 76 and 205 mm (3 and 8") with launch velocities of 68, 91 and 113.6 m/s (225, 300 and 375 ft/s) (–20%, typical and +20%) (2500 ft above sea level, 550° C, 50% RH).

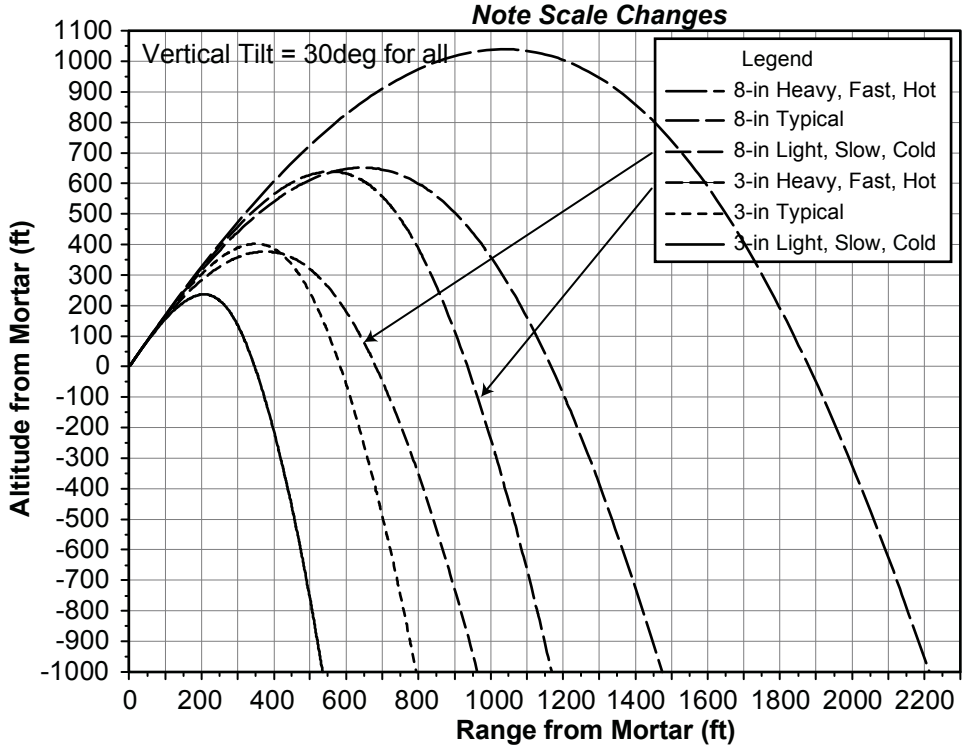

Figure 14. Comparison of trajectories for 76 and 205 mm (3 and 8") with extreme mass, velocity and altitude.